

PMMA: The Polytechnique Montréal Mobility Aids Dataset

Qingwu Liu, Nicolas Saunier, and Guillaume-Alexandre Bilodeau ^{*}

February 12, 2026

Abstract

This study introduces a new object detection dataset of pedestrians using mobility aids, named PMMA. The dataset was collected in an outdoor environment, where volunteers used wheelchairs, canes, and walkers, resulting in nine categories of pedestrians: pedestrians, cane users, two types of walker users, whether walking or resting, five types of wheelchair users, including wheelchair users, people pushing empty wheelchairs, and three types of users pushing occupied wheelchairs, including the entire pushing group, the pusher and the person seated on the wheelchair. To establish a benchmark, seven object detection models (Faster R-CNN, CenterNet, YOLOX, DETR, Deformable DETR, DINO, and RT-DETR) and three tracking algorithms (ByteTrack, BOT-SORT, and OC-SORT) were implemented under the MMDetection framework. Experimental results show that YOLOX, Deformable DETR, and Faster R-CNN achieve the best detection performance, while the differences among the three trackers are relatively small. The PMMA dataset is publicly available at: <https://doi.org/10.5683/SP3/XJPQUG> and the video processing and model training code is available at: <https://github.com/DatasetPMMA/PMMA>.

Keywords: Computer vision, image processing, pedestrian flows and crowds, mobility aids, object detection and tracking dataset

^{*}Qingwu Liu and Nicolas Saunier are from Civil, Geological and Mining Engineering Department, Guillaume-Alexandre Bilodeau is from Computer Engineering and Software Engineering Department, Polytechnique Montréal, 2500 Chem. de Polytechnique, Montréal, Canada, H3T 1J4. Contact: qingwu.liu@polymtl.ca, nicolas.saunier@polymtl.ca and guillaume-alexandre.bilodeau@polymtl.ca

1 Introduction

Cameras have become ubiquitous in traffic environments, serving as essential tools for capturing and analyzing road users to better understand their behaviors and anticipate their movements. In both computer vision and intelligent transportation systems, object detection and tracking are fundamental tasks. Existing publicly available object detection and tracking datasets classify road users into broad categories such as pedestrians, cyclists, cars and trucks. However, few datasets provide finer-grained distinctions among pedestrians, particularly pedestrians who use mobility aids such as wheelchairs, walkers, or canes. Although individuals using mobility aids represent a small fraction of road users, they are more vulnerable than other groups. This underscores the need for dedicated datasets that specifically identify mobility aid users and enable a thorough evaluation of state-of-the-art (SOTA) detection and tracking algorithms. Such efforts are crucial for advancing inclusive and safety-focused intelligent transportation systems.

Image-based object detection and tracking methods have seen significant progress, driven not only by the advancement of computational power, the increase of GPU resources, but also by the evolution of deep learning models, such as convolutional neural networks (CNN) [1] and Transformers [2], the availability of large-scale annotated datasets, and improved training techniques. These advancements have enabled SOTA models to achieve strong performance on public datasets such as COCO [3], KITTI [4], and Cityscapes [5]. However, due to the limited category granularity in existing datasets, how these methods perform when faced with multiple visually similar categories remains an open question.

Therefore, we introduce in this paper our mobility aids dataset, which contains over 28,000 annotated images with a resolution of 2208×1242 pixels and a maximum frame rate of 15 frames per second (fps). We collected the dataset using a ZED 2 stereo camera in an outdoor parking lot of Polytechnique Montréal, located in Montréal, Québec, Canada. Three videos were annotated from two points of view with nine categories of pedestrians using computer vision annotation tools (CVAT) [6], as visualized in Figure 1. We compare our dataset with existing object detection datasets in Table 1.

To evaluate the performance of detectors and trackers in our dataset, we benchmark seven detectors and three trackers on our dataset. We further discuss their performance and the shortcomings. Finally, we summarize the most challenging categories and the limitations of those methods on our dataset.

The main contributions of this study are summarized as follows:



Figure 1: Example frames of our Mobility Aids Dataset. There are nine categories, with detailed descriptions in Table 3 and icons adapted from [7,8]

1. We constructed a dataset containing nine categories of pedestrians with mobility aids, with annotations provided for all images and oc-

clusion information recorded for each annotated instance;

2. We applied seven object detection methods and three tracking methods on the dataset; and
3. We analyzed the experimental results and highlighted the main challenges associated with the detection and tracking of pedestrians using mobility aids.

The remainder of this paper is organized as follows. Section 2 presents the related work. Section 3 introduces the details of our dataset. Section 4 presents the experimental protocol and evaluation metrics. Section 5 presents the results and the discussion, and section 6 concludes the paper.

2 Related Work

In this section, prior datasets and data collection paradigms relevant to our work are reviewed. We begin by discussing autonomous-driving datasets collected from vehicle-mounted sensors, which provide rich annotations but remain limited by car-centric visibility and short sequence durations. We then review fixed-camera and multi-camera surveillance datasets that offer high-density pedestrian tracking from elevated viewpoints. Finally, we highlight datasets that, similar to ours, focus on fine-grained pedestrian sub-categories, particularly those involving mobility aids.

Several widely used datasets in the autonomous driving domain have been collected using vehicle-mounted sensors. Notable examples include KITTI [4], Waymo Open Dataset [9], SemanticKITTI [10], JAAD [11], nuScenes [12], and Cityscapes [5]. These datasets provide high-quality sensor data, such as LiDAR and RGB images, collected as vehicles drive through urban environments. The low camera position and occlusions by other vehicles limit visibility, and most of the data is captured in multiple short-duration segments, typically lasting only a few seconds. Even with longer sequences, detailed traffic analysis remains challenging due to the inherent limitations of the vehicle perspective. In addition, although these datasets are useful for tasks, such as object detection and semantic segmentation in road scenes, they mainly focus on general object categories, such as pedestrians, cars, and cyclists, without distinguishing between pedestrians with or without mobility aids.

In crowded public spaces, several datasets focus on fixed-camera surveillance or multi-camera scenarios. MOT20 [13] offers high-density pedestrian tracking sequences from viewpoints at lamppost or building height. The

A9-Dataset [14] provides high-resolution multi-modal data collected from roadside sensor infrastructure along a three kilometers stretch of the A9 autobahn near Munich, Germany. It includes precision-timestamped camera and LiDAR frames captured from overhead gantry bridges, with objects annotated using 3D bounding boxes. WILDTRACK [15] and CityFlow [16] are multi-view datasets that allow for 3D localization and multi-camera tracking. LUMPI [17] is another multi-perspective dataset designed for analyzing pedestrian behavior across viewpoints. While these datasets provide multi-angle coverage and dense pedestrian annotations, they do not include detailed pedestrian categories either.

Similar to our dataset, a few datasets categorize pedestrians into multiple subclasses to enable fine-grained analysis. SynPoses [18] proposes a framework for generating high-quality synthetic human data with diverse and complex poses, addressing the limited pose variability in existing real-world datasets. RAP [19] is a large-scale pedestrian dataset designed for person retrieval in real surveillance environments, featuring rich attribute annotations and identity labels that enable both attribute-based and image-based person re-identification. The dataset mainly focuses on appearance-related attributes, such as clothing styles and hair characteristics, while mobility-aid users are not explicitly considered. A few datasets explicitly consider categories related to mobility aids. For instance, the dataset proposed by Sonia Dávila-Soberón et al. [20] specifically focuses on wheelchair users, cane users, and the mobility aids themselves. However, this dataset is not publicly available, which limits its accessibility for broader research purposes. Another dataset [21] targets mobility aid users in an indoor hospital environment, providing valuable data for healthcare-related applications but lacking outdoor scene variability and typical viewpoints. In addition, Zhang et al. [22] introduced a synthetic dataset in a simulation environment called X-World, which includes objects such as wheelchairs and canes. While useful for controlled experiments, simulation-based data often lacks the complexity and diversity of real-world environments.

To the best of our knowledge, there is currently no publicly available dataset that captures in real-world outdoor conditions people using diverse mobility aids, such as wheelchairs, walkers and canes, while also supporting tasks like object detection and multi-object tracking (MOT). This highlights a gap in existing datasets for developing and evaluating vision-based systems that aim to understand and assist mobility-impaired individuals in dynamic, open outdoor environments.

Table 1: Comparison of the PMMA dataset statistics with existing benchmarks

Dataset	View	Images	Categories with persons	Outdoor	Real world	Mobility Aids
Vehicle-perspective						
KITTI [4]	ego	15k	3	✓	✓	✗
Waymo [9]	ego	1M	2	✓	✓	✗
Cityscapes [5]	ego	25k	2	✓	✓	✗
JAAD [11]	ego	346k	1	✓	✓	✗
nuScenes [12]	ego	1.4M	2	✓	✓	✗
Multi-perspective						
WILDTRACK [15]	surv+ego	215k	1	✓	✓	✗
CityFlow [16]	surv+surv	118k	2	✓	✓	✗
A9-Dataset [14]	surv	5.4k	3	✓	✓	✗
LUMPI [17]	surv+ego	200k	3	✓	✓	✗
Detailed categories						
Sonia Dávila-Soberón et al. [20]	surv	2.8k	3	✓	✓	✓
Indoor hospital [21]	ego	17k	5	✗	✓	✓
X-world [22]	surv	72k	6	✓	✗	✓
PMMA (Ours)	surv	28k	9	✓	✓	✓

Notes: surv and ego denote surveillance and vehicle-mounted views, respectively.

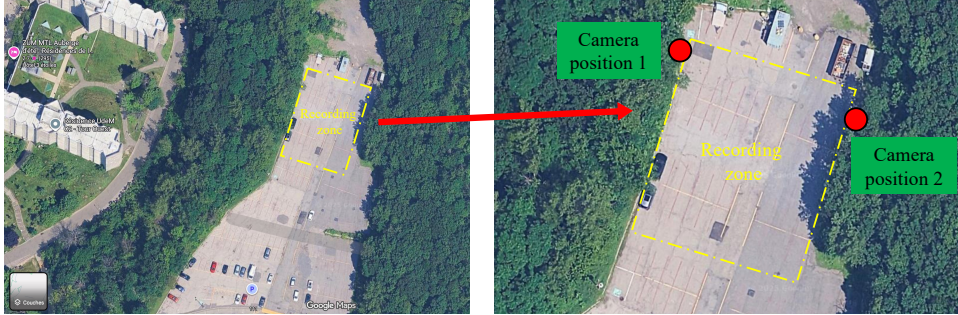


Figure 2: Data collection area in the parking lot of Polytechnique Montréal

3 The PMMA Dataset

3.1 Data Collection

3.1.1 Acquisition and Ethics

The data collection for this dataset was approved by the ethics committee (“Comité d’éthique à la recherche avec des êtres humains”) of Polytechnique Montréal. All participants were volunteers who consented to be filmed and have their data included in the dataset. None of the participants are actual users of mobility aids; instead, they are graduate students performing scenarios to simulate behaviors with mobility aids. Volunteers change and use different mobility aids within each session.

3.1.2 Location

The dataset was recorded from two camera positions in an outdoor parking lot of Polytechnique Montréal, in Montréal, Québec, Canada. The recording zone captured from Google Maps is shown in Figure 2. We focus on the area delineated by traffic cones, which marks the boundary of the region of interest in the scene, highlighted in Figure 1.

3.1.3 Camera

The dataset was recorded utilizing a stereo camera ZED 2 [23]. It provides dual streams in a side-by-side configuration with resolution 2208×1242 at 15 frame per second (fps) and has a maximum field of view (FOV) of horizontal \times vertical \times diagonal angles of $110^\circ \times 70^\circ \times 120^\circ$. The camera was mounted on a 4-m-high pole, which was mounted on two distinct streetlight poles



Figure 3: Illustration of the camera and the pole

giving two separate viewpoints: one of the installations is shown in Figure 3. A Linux system laptop was used to record the video stream from the camera via the VLC media player [24].

3.1.4 Recording sessions

Three recording sessions were conducted on the same day. The sunlight varies throughout the recording period due to partially cloudy weather conditions. The recording sessions are summarized in Table 2.

3.1.5 Object categories

The mobility aids utilized in this data collection includes three wheelchairs, two walkers and two canes. With these mobility aids, the dataset includes nine pedestrian categories, representing a variety of mobility aids and users, shown in Table 3. Going into details, the walker category is further refined into two subcategories based on the activity status, walking or resting. These subcategories allow for more fine-grained behavior analysis, though they can be easily merged into a single walker category if needed. For

wheelchair-related instances, we introduce a more structured annotation strategy. Specifically, we consider a wheelchair and the associated person(s) as a single unit and classify them into five distinct subcategories: a person alone in a wheelchair, a person pushing an empty wheelchair, a person pushing a person in a wheelchair as a group and its components separately, the person pushing and the seated person.

This hierarchical categorization allows us to model complex pedestrian interactions and mobility aid usage more accurately, while maintaining the flexibility to merge classes as needed for specific tasks or evaluation protocols.

3.2 Annotation

3.2.1 Video pre-processing

Each stereo video is saved to a sequence of stereo images firstly. Each stereo image is then separated into left and right images, and the left images are annotated.

3.2.2 Annotation tool

We use the computer vision annotation tool (CVAT) [6], which is an online platform for annotating object detection and tracking. The annotations are in the COCO format to facilitate model training and evaluation.

3.2.3 Annotation details

The annotations were separated into three tasks with respect to the three capture sessions. The annotations were initially generated by labelling key frames at every 100 frames using the interpolation-based tracking tool. Linear interpolation was applied between key frames to estimate intermediate object locations, followed by manual frame-by-frame corrections to ensure accuracy.

We also include occlusion attributes in the annotations. Following common occlusion conventions, such as those used in KITTI [4], we assign labels 0, 1, and 2 to represent no occlusion, partial occlusion, and full occlusion, respectively. Additionally, we introduce an extra label, 3, to indicate objects in the tree shadows, which is not defined in the original KITTI annotation scheme.

Table 2: Details of the collected video recordings

Recording session	Duration	FPS	Position	Number of Frames
Video 1	10 min	15	1	9,000
Video 2	10 min	15	1	5,000
Video 3	15 min	13	2	14,637

Table 3: Description of pedestrian-related categories

Icon	Category	Description
	Ped	Pedestrian without mobility aid
	Cane	Pedestrian using a cane
	Wheelchair	Person in a self-propelled wheelchair
	WalkerWalking	Person walking with a walker
	WalkerResting	Person resting with a walker
	PushEmptyWheelchair	Person pushing an empty wheelchair
	WheelchairGroup	Person pushing a person in a wheelchair as a group
	WheelchairPusher	Person pushing only (from WheelchairGroup)
	WheelchairPushedUser	Person in a wheelchair only (from WheelchairGroup)

Table 4: Frame distribution across training, validation, and test sets from different video sources

Video	Train		Validation		Test	
	Video 1	Video 3	Video 2	Video 3	Video 2	Video 3
Number	9,000	13,248	1,700	534	4,357	799
Total		22,248		2,234		5,156

Table 5: Comparison of object detection models

Model	Type	Stage	Anchor-free	Backbone
Faster R-CNN [25]	CNN	Two-stage	No	ResNet-50
CenterNet [26]	CNN	One-stage	Yes	Hourglass
YOLOX [27]	CNN	One-stage	Yes	CSPDarknet
DETR [28]	Transformer	One-stage	Yes	ResNet-50
Deformable DETR [29]	Transformer	One-stage	Yes	ResNet-50
DINO [30]	Transformer	One-stage	Yes	ResNet-50
RT-DETR [31]	Transformer	One-stage	Yes	ResNet-50

3.3 Statistics

Around 30,000 images were annotated in our PMMA dataset. Figure 4 illustrates the annotation counts for each category per video. The frame distributions for the training, validation and test sets are shown in Table 4. For the tracking task, the two video clips in the test set are used to evaluate the tracker performance.

4 Experimental Methodology

4.1 Introduction

To establish baseline performance on our dataset, we conducted a series of experiments comparing the performance of object detection and MOT methods. For object detection, we used the MMDetection [32] framework and selected seven representative methods: Faster R-CNN [25], CenterNet [26], YOLOX [27], DETR [28], Deformable DETR [29], DINO [30] and RT-DETR [31], as summarized in Table 5. All models were pretrained on the COCO dataset and then trained on our dataset to evaluate their detection performance across the nine pedestrian-related categories.

For MOT, we applied three trackers, including ByteTrack [33], BOT-

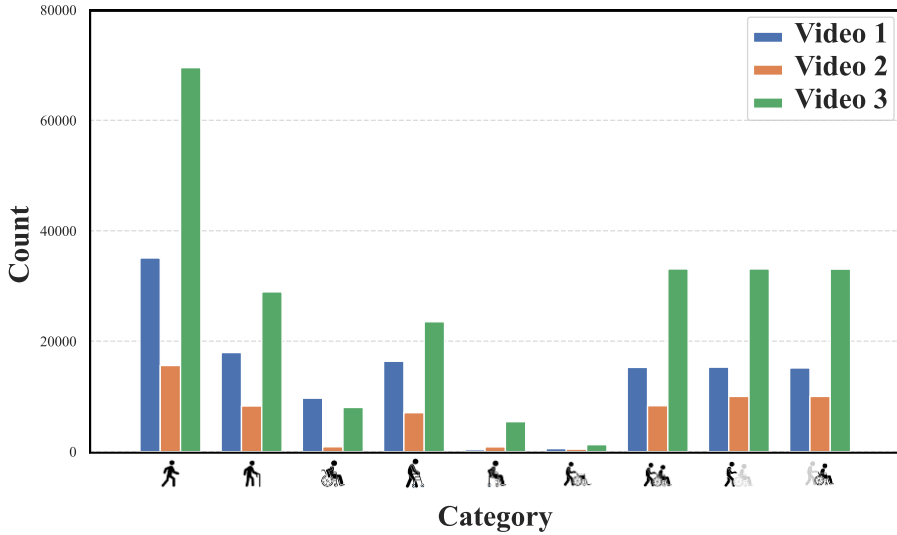


Figure 4: Category-wise annotation counts for each video

SORT [34] and OC-SORT [35], on the detection results, as summarized in Table 6. This experimental setup allows us to establish baseline detection and tracking performance on the dataset and provides a reference for future research using our data.

For object detection, we trained for 50 epochs and we use early-stopping. We used an AdamW [36] optimizer with a learning rate of 1×10^{-4} and a weight decay of 1×10^{-4} .

4.2 Evaluation Metrics

4.2.1 Object Detection

We evaluated the performance of the detection methods using the standard COCO metrics [37]:

- **mAP:** The mean of average precision (AP), where AP is computed by integrating the precision–recall curve at a fixed IoU threshold, measuring overall detection performance.
- **AP₅₀:** Average precision over multiple recall levels at an Intersection over Union (IoU) threshold of 0.5, measuring detection accuracy when predicted boxes overlap with ground truth by at least 50%.

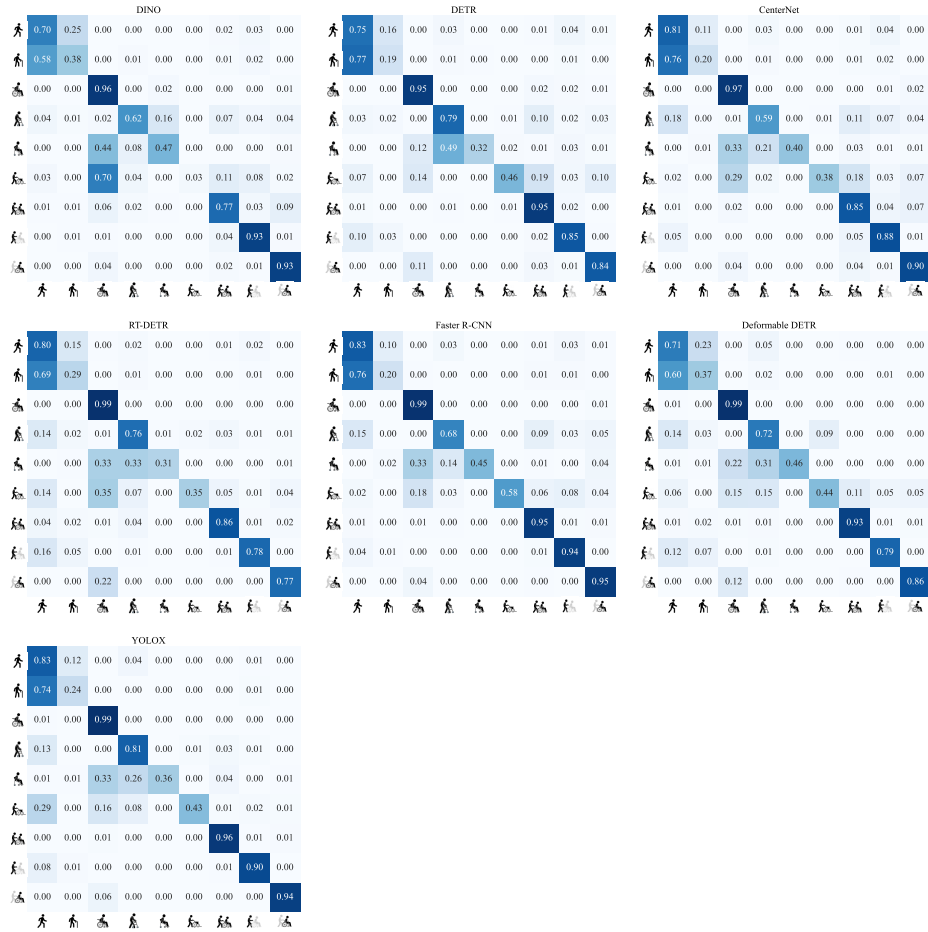


Figure 5: Row-normalized confusion matrices of all detection methods on the test set. Each row and column represent the ground truth (GT) and predicted classes, respectively

- **AP₇₅**: Average precision over multiple recall levels at an IoU threshold of 0.75, reflecting stricter overlap criteria for more precise detections.
- **AP_S, AP_M, AP_L**: Average precision scores over multiple recall levels for small (area $\leq 32^2$ pixels), medium ($32^2 < \text{area} < 96^2$ pixels), and large ($\geq 96^2$ pixels) objects, respectively, assessing performance across different object scales.
- **mAR**: The mean average recall over multiple IoU thresholds, indicating the model’s ability to find all relevant objects.
- **AR_S, AR_M, AR_L**: Average recall for small, medium, and large objects, respectively, where the object size definitions are the same as those used for AP_S, AP_M, and AP_L.
- **mAP** and **mAR** are also reported across different occlusion levels, including no occlusion, partial occlusion, and full occlusion. Objects in shadows are included in the Full occlusion category.

All evaluation metrics are reported for the overall performance across the nine categories, whereas for the category-wise analysis, only mAP, AP₅₀, and AP₇₅ are presented.

4.2.2 Object Tracking

We adopted the Higher Order Tracking Accuracy (HOTA) metric [38] for each test set. HOTA is a comprehensive metric that jointly considers detection accuracy (Deta), association accuracy (AssA), and localization accuracy (LocA). HOTA is defined as follows:

$$\text{HOTA}_\alpha = \sqrt{\frac{\sum_{c \in \{\text{TP}\}} \mathcal{A}(c)}{|\text{TP}| + |\text{FN}| + |\text{FP}|}} \quad (1)$$

where |TP|, |FN|, and |FP| denote the number of true positives, false negatives, and false positives, respectively. Each c represents a true positive match between a ground truth ID and a predicted ID. $\mathcal{A}(c)$ denotes the *association accuracy* of match c , which is defined as:

$$\mathcal{A}(c) = \frac{|\text{TPA}(c)|}{|\text{TPA}(c)| + |\text{FNA}(c)| + |\text{FPA}(c)|} \quad (2)$$

where |TPA(c)|, |FNA(c)|, and |FPA(c)| refer to the number of true positive, false negative, and false positive associations related to match c , respectively.

Table 6: Comparison of tracking methods (Re-ID refers to the use of appearance-based features to associate detections across frames, enabling identity recovery after occlusion or long-term target loss.)

Model	Re-ID	Detection-based Tracking
ByteTrack [33]	No	Yes
BOT-SORT [34]	Yes	Yes
OC-SORT [35]	No	Yes

Table 7: Detection performance evaluated on the test set across all categories

Method	mAP(%)	AP ₅₀ (%)	AP ₇₅ (%)	AP _S (%)	AP _M (%)	AP _L (%)	mAR(%)	AR _S (%)	AR _M (%)	AR _L (%)
DINO	27.8	55.6	24.1	7.2	24.9	42.2	57.5	9.9	53.2	73.1
DETR	30.4	60.7	26.7	0.0	29.7	38.6	45.4	0.3	44.8	52.7
RT-DETR	40.0	59.3	48.6	19.3	38.1	43.0	47.3	21.3	44.8	51.1
CenterNet	44.4	67.7	52.5	46.9	48.9	<u>45.0</u>	<u>60.7</u>	<u>47.0</u>	62.6	61.4
Deformable DETR	47.4	<u>68.4</u>	<u>58.4</u>	22.2	50.4	42.6	64.7	54.4	65.5	64.5
Faster R-CNN	49.4	73.9	<u>60.5</u>	<u>19.8</u>	51.5	49.5	<u>58.8</u>	21.9	59.8	<u>59.5</u>
YOLOX	49.5	69.5	61.9	14.8	<u>49.9</u>	49.0	57.4	<u>32.8</u>	<u>58.8</u>	56.0

Notes: **Bold**, *italic*, and underline represent the first, second, and third best performances, respectively. Methods are sorted based on mAP. These notational conventions apply to all the following tables in this paper.

Table 8: Detection performance for each of the nine categories on the test set

Method	Ped			Cane			Wheelchair		
	mAP(%)	AP ₅₀ (%)	AP ₇₅ (%)	mAP(%)	AP ₅₀ (%)	AP ₇₅ (%)	mAP(%)	AP ₅₀ (%)	AP ₇₅ (%)
DETR	23.1	51.7	16.4	4.7	11.2	3.1	51.1	76.8	63.6
DINO	27.8	58.1	22.6	9.0	26.5	5.3	34.9	66.0	20.0
RT-DETR	37.2	60.6	41.1	<u>9.2</u>	16.3	9.8	59.0	78.7	73.7
Faster R-CNN	36.5	61.3	38.9	8.7	16.6	7.8	<u>62.2</u>	<u>86.4</u>	<u>79.4</u>
CenterNet	<u>38.5</u>	<u>63.1</u>	<u>42.0</u>	<u>10.2</u>	<u>18.9</u>	<u>9.5</u>	46.0	62.7	61.1
Deformable DETR	<u>39.7</u>	<u>62.3</u>	<u>47.3</u>	14.0	<u>26.0</u>	13.9	69.5	87.7	86.9
YOLOX	44.1	66.2	53.7	8.8	16.2	9.0	72.2	88.9	88.4
Method	WalkerWalking			WalkerResting			PushEmptyWheelchair		
	mAP(%)	AP ₅₀ (%)	AP ₇₅ (%)	mAP(%)	AP ₅₀ (%)	AP ₇₅ (%)	mAP(%)	AP ₅₀ (%)	AP ₇₅ (%)
DINO	8.4	12.4	11.1	39.1	68.6	42.4	12.7	38.0	2.3
DETR	24.1	43.7	23.7	37.6	71.0	38.1	24.3	44.7	27.8
RT-DETR	25.7	35.8	34.0	<u>48.0</u>	<u>73.3</u>	56.1	21.6	35.2	25.8
CenterNet	<u>41.4</u>	<u>55.0</u>	<u>54.2</u>	47.9	<u>70.7</u>	<u>56.4</u>	<u>35.4</u>	<u>60.9</u>	38.8
Deformable DETR	23.8	33.1	30.3	45.6	73.1	50.9	<u>40.5</u>	<u>55.8</u>	52.4
YOLOX	<u>34.4</u>	<u>46.9</u>	<u>44.3</u>	53.9	79.5	62.6	27.3	39.5	<u>38.9</u>
Faster R-CNN	52.2	71.6	70.3	48.6	77.7	56.9	44.2	61.3	58.6
Method	WheelchairGroup			WheelchairPusher			WheelchairPushedUser		
	mAP(%)	AP ₅₀ (%)	AP ₇₅ (%)	mAP(%)	AP ₅₀ (%)	AP ₇₅ (%)	mAP(%)	AP ₅₀ (%)	AP ₇₅ (%)
DETR	42.2	91.5	25.4	26.3	73.5	11.3	40.7	82.4	30.8
DINO	51.9	80.4	64.8	30.7	68.9	23.9	35.9	81.6	24.0
RT-DETR	60.8	79.9	77.4	47.3	75.5	55.6	50.7	78.1	63.9
CenterNet	68.7	92.2	85.0	56.5	92.5	64.2	55.1	93.0	61.2
Deformable DETR	<u>72.0</u>	<u>94.8</u>	<u>91.7</u>	<u>57.6</u>	89.8	<u>69.6</u>	<u>64.3</u>	<u>93.3</u>	82.3
Faster R-CNN	<u>74.0</u>	<u>97.1</u>	<u>93.3</u>	58.5	95.9	<u>68.0</u>	<u>59.7</u>	<u>97.3</u>	<u>71.7</u>
YOLOX	74.4	98.3	95.0	59.9	<u>92.3</u>	74.0	70.8	97.6	90.9

Specifically, we report HOTA along with DetA, AssA, and LocA, presenting both the overall performance across all nine categories and the category-wise performance. We also include the total number of detected objects and tracked identities.

5 Results and Discussion

5.1 Object Detection

The object detection performance across all categories is given in Table 7. YOLOX, Deformable DETR, and Faster R-CNN achieve the top three performances across most metrics. Specifically, YOLOX has the best AP while Deformable DETR has the best AR. However, the performance differences among CenterNet, RT-DETR, Faster R-CNN, Deformable DETR, and YOLOX are relatively small, whereas DINO and DETR lag significantly behind the other five.

Moreover, the object detection performance for each category is given in Table 8. YOLOX, Deformable DETR, and Faster R-CNN achieve the best performance. CenterNet performs comparably well to these three methods. DETR and DINO consistently exhibit the lowest performance.

Regarding the categories, cane users are the most challenging to detect. This could be attributed to the fact that the cane, being a thin object, is difficult to detect and cane users are therefore confused with pedestrians without any mobility aid. Wheelchair-related categories achieve higher mAP and mAR; however, PushEmptyWheelchair shows the lowest accuracy among them, possibly due to its visual similarity to WheelchairGroup. Figure 5 shows that the confusion matrices on the test set are similar for all the methods. There is substantial confusion (1) between pedestrians without any mobility aid and cane users, and (2) between wheelchair users and walker users.

Table 9 presents the detection results with respect to different occlusion levels. DINO has the best mAP in case of no occlusion and poor performance on the partial and full occlusion cases. Generally, Faster R-CNN, Deformable DETR and YOLOX have the top performance consistent with the overall detection results.

5.2 Object Tracking

Based on the detection performance, we applied three tracking algorithms to the top five methods, excluding DINO and DETR. We report the ob-

Table 9: Detection results on the test set with respect to different occlusion levels

Methods	mAP(%)			mAR(%)		
	No	Partial	Full	No	Partial	Full
DETR	45.20	10.34	8.33	70.56	72.63	63.38
CenterNet	50.99	<u>12.37</u>	10.04	<u>76.79</u>	<u>84.42</u>	<u>75.04</u>
RT-DETR	52.50	11.28	11.19	71.87	69.35	73.82
Deformable DETR	53.83	11.91	<u>10.89</u>	70.32	69.36	68.25
Faster R-CNN	<u>54.10</u>	<u>13.03</u>	10.79	81.85	88.36	81.02
YOLOX	55.98	13.38	<u>11.05</u>	80.22	<u>85.28</u>	<u>78.11</u>
DINO	57.06	10.56	5.72	57.56	48.73	29.48

ject tracking results on overall performance and per-category performance separately on videos 2 and 3 from the test set in Table 10.

For overall performance, among the detectors, YOLOX achieves the best HOTA on video 2, while Deformable DETR performs best on video 3. Among the trackers, ByteTrack consistently outperforms the others on both videos, though the differences between the three trackers are relatively small and OC-SORT with Faster R-CNN on video 2 and BOT-SORT with Deformable DETR on video 3 show good performance. All trackers show strong DetA and LocA. The AssA for video 2 is relatively low, primarily because the tracker generates more IDs than the ground truth objects, resulting in a reduced overall HOTA score.

The category-wise performances are summarized in Tables 11 to 16. On video 2, the performance of all methods on the categories Cane, Walker-Resting, and PushEmptyWheelchair is lower than 10 %; The performance on the categories Ped and WalkerWalking is between 10 % and 40 %; the performance on Wheelchair, WheelchairGroup, WheelchairPusher and WheelchairPushedUser is the highest, with the best performance over 40 %. YOLOX and Deformable DETR have quite close performance. On video 3, all the methods perform better on Ped, Cane, Wheelchair, Wheelchair-Group, WheelchairPusher and WheelchairPushedUser, with the best performance over 60 %. Deformable DETR and YOLOX demonstrate the strongest overall performance across most mobility-related categories. On Video 2, Deformable DETR ranks within the top three for 6 of the 9 categories, while YOLOX achieves top-three performance in all 9 categories. On Video 3, Deformable DETR attains top-three results in 8 of the 8 eval-

Table 10: Tracking performance across different detectors and trackers for all categories on videos 2 and 3 from the test set, sorted by HOTA

Detector	Method	Video 2				Detection Counts		Track ID Counts	
		Tracking Metrics (%)				Predictions	GT	Predictions	GT
		HOTA	DetA	AssA	LocA				
Deformable DETR	OC-SORT	32.41	62.63	16.92	84.82	53,970		453	
CenterNet	OC-SORT	33.38	63.16	17.80	83.69	63,446		617	
CenterNet	BOT-SORT	34.10	60.35	19.43	83.54	74,418		1,543	
RT-DETR	OC-SORT	34.14	63.60	18.50	82.87	60,730		468	
RT-DETR	BOT-SORT	35.62	62.82	20.36	82.6	67,962		1,075	
RT-DETR	ByteTrack	35.87	63.74	20.36	82.83	66,914		584	
CenterNet	ByteTrack	36.27	61.29	21.61	83.75	72,990		668	
Deformable DETR	BOT-SORT	37.88	67.68	21.36	84.43	64,415	64,678	1,125	35
Deformable DETR	ByteTrack	39.00	68.03	22.55	84.7	63,348		499	
Faster R-CNN	BOT-SORT	44.54	60.85	32.86	83.27	76,882		1,053	
Faster R-CNN	ByteTrack	45.34	61.76	33.59	83.27	75,869		527	
Faster R-CNN	OC-SORT	46.39	63.70	34.12	83.39	70,059		466	
YOLOX	BOT-SORT	52.62	67.93	41.02	85.02	71,718		910	
YOLOX	OC-SORT	53.02	70.07	40.38	85.14	65,796		407	
YOLOX	ByteTrack	54.91	68.59	44.23	85.21	70,864		451	
Video 3									
Detector	Method	Tracking Metrics (%)				Detection Counts		Track ID Counts	
		HOTA	DetA	AssA	LocA	Predictions	GT	Predictions	GT
CenterNet	OC-SORT	55.41	69.85	44.13	94.94	13,634		101	
CenterNet	BOT-SORT	62.50	65.34	59.97	84.89	15,374		290	
CenterNet	ByteTrack	65.70	66.19	65.47	84.7	15,129		108	
Faster R-CNN	OC-SORT	66.89	74.43	60.38	86.02	13,490		71	
RT-DETR	OC-SORT	69.08	76.16	63.12	85.54	12,941		47	
Faster R-CNN	BOT-SORT	70.88	72.66	69.43	86.06	14,232		187	
Faster R-CNN	ByteTrack	72.45	73.37	71.80	86.05	14,072		94	
YOLOX	ByteTrack	72.97	77.20	69.32	85.89	13,142	12,784	84	17
YOLOX	BOT-SORT	73.30	76.54	70.58	85.93	13,284		168	
Deformable DETR	OC-SORT	73.48	79.73	68.00	87.06	12,373		36	
YOLOX	OC-SORT	74.08	78.07	70.68	85.95	12,756		70	
RT-DETR	BOT-SORT	77.56	75.82	79.85	85.47	13,431		115	
RT-DETR	ByteTrack	77.71	76.23	79.70	85.43	13,333		52	
Deformable DETR	BOT-SORT	79.30	80.50	78.38	87	12,747		71	
Deformable DETR	ByteTrack	79.42	80.53	78.57	86.98	12,691		34	

Note: Methods are sorted based on HOTA in this table and the following ones.

uated categories, and YOLOX performs similarly with 7 top-three finishes. Overall, the performance differences among the trackers are relatively small; detection accuracy remains the key factor influencing tracking performance.

6 Conclusion

In this study, we collected a mobility aids dataset, named PMMA, and used it to benchmark SOTA detection and tracking methods. PMMA contains high-resolution videos with annotations for nine mobility-aid-related categories, including pedestrians, cane users, two types of walker users (walk-

ing and resting), five types of wheelchair users, including wheelchair users, people pushing empty wheelchairs, and three types from wheelchair groups (Wheelchair group, wheelchair pusher and wheelchair user together with wheelchair). The dataset was divided into training, validation, and test sets. We evaluated seven object detectors, including Faster R-CNN, Center-Net, YOLOX, DETR, Deformable DETR, DINO, and RT-DETR, and applied three MOT trackers, namely ByteTrack, BOT-SORT, and OC-SORT, on the top five detection models. We reported both overall and category-wise performance. The results show that YOLOX, Deformable DETR, and Faster R-CNN achieved the best detection performance, while the differences among the three trackers were small. In terms of categories, Wheelchair, WheelchairGroup, WheelchairPusher, and WheelchairPushedUser were the easiest to detect and track, whereas performance for the remaining categories was less stable and strongly influenced by the specific scenarios.

Overall, YOLOX, Deformable DETR, and Faster R-CNN achieved the best performance among the seven evaluated methods. They performed well on wheelchair-related categories. However, performance on the other categories varies significantly across different scenarios. The differences among the three trackers were minimal, as their results largely depended on the quality of the detections. Nevertheless, no single method performed well across all nine categories, highlighting the ongoing challenge of automatic data collection of mobility aid users. Transportation studies focusing on these users still require improving detection and tracking accuracy.

Acknowledgments

The authors gratefully acknowledge financial support from the China Scholarship Council, as well as the financial support of NSERC through the Discovery Grant 2023-05626. The authors would also like to thank the Interuniversity Research Centre on Enterprise Networks, Logistics and Transportation (CIRRELT) for the computing servers and to NVIDIA Corporation for providing GPUs. This research was also enabled in part by support the computing resources provided by Digital Research Alliance of Canada.

References

- [1] A. Krizhevsky, I. Sutskever, and G. E. Hinton, “Imagenet classification with deep convolutional neural networks,” in *Advances in neural information processing systems (NeurIPS)*, 2012, pp. 1097–1105.

- [2] A. Vaswani, N. Shazeer, N. Parmar, J. Uszkoreit, L. Jones, A. N. Gomez, L. Kaiser, and I. Polosukhin, “Attention is all you need,” in *Advances in neural information processing systems (NeurIPS)*, 2017, pp. 5998–6008.
- [3] T.-Y. Lin, M. Maire, S. Belongie, J. Hays, P. Perona, D. Ramanan, P. Dollár, and C. L. Zitnick, “Microsoft coco: Common objects in context,” in *European conference on computer vision*. Springer, 2014, pp. 740–755.
- [4] A. Geiger, P. Lenz, and R. Urtasun, “Are we ready for autonomous driving? the kitti vision benchmark suite,” in *Conference on Computer Vision and Pattern Recognition (CVPR)*, 2012.
- [5] M. Cordts, M. Omran, S. Ramos, T. Rehfeld, M. Enzweiler, R. Benenson, U. Franke, S. Roth, and B. Schiele, “The cityscapes dataset for semantic urban scene understanding,” in *Conference on Computer Vision and Pattern Recognition (CVPR)*. IEEE, 2016, pp. 3213–3223.
- [6] CVAT.ai Corporation, “Computer Vision Annotation Tool (CVAT),” Nov. 2023. [Online]. Available: <https://github.com/cvcat-ai/cvat>
- [7] Karyative, “Physiotherapy icons,” <https://www.flaticon.com/free-icons/physiotherapy>, 2025, accessed: 2025-04-02.
- [8] Leremy, “Wheelchair icons,” Flaticon, 2025. [Online]. Available: <https://www.flaticon.com/free-icons/wheelchair>
- [9] P. Sun, H. Kretzschmar, X. Dotiwalla, A. Chouard, V. Patnaik, P. Tsui, J. Guo, Y. Zhou, Y. Chai, B. Caine, V. Vasudevan, W. Han, J. Ngiam, H. Zhao, A. Timofeev, S. Ettinger, M. Krivokon, A. Gao, A. Joshi, Y. Zhang, J. Shlens, Z. Chen, and D. Anguelov, “Scalability in perception for autonomous driving: Waymo open dataset,” in *Proceedings of the IEEE/CVF Conference on Computer Vision and Pattern Recognition (CVPR)*, June 2020.
- [10] J. Behley, M. Garbade, A. Milioto, J. Quenzel, S. Behnke, C. Stachniss, and J. Gall, “SemanticKITTI: A Dataset for Semantic Scene Understanding of LiDAR Sequences,” in *Proc. of the IEEE/CVF International Conf. on Computer Vision (ICCV)*, 2019.
- [11] A. Rasouli, I. Kotseruba, and J. K. Tsotsos, “Jaad: A large-scale dataset for joint attention in autonomous driving,” *IEEE Transactions on Intelligent Transportation Systems*, vol. 19, no. 2, pp. 458–470, 2018.

- [12] H. Caesar, V. Bankiti, A. H. Lang, S. Vora, V. E. Liong, Q. Xu, A. Krishnan, Y. Pan, G. Baldan, and O. Beijbom, “nuscenes: A multimodal dataset for autonomous driving,” 2020. [Online]. Available: <https://arxiv.org/abs/1903.11027>
- [13] P. Dendorfer, H. Rezatofighi, A. Milan, J. Shi, D. Cremers, I. Reid, S. Roth, K. Schindler, and L. Leal-Taixé, “Mot20: A benchmark for multi object tracking in crowded scenes,” 2020. [Online]. Available: <https://arxiv.org/abs/2003.09003>
- [14] C. Creß, W. Zimmer, L. Strand, M. Fortkord, S. Dai, V. Lakshminarasimhan, and A. Knoll, “A9-dataset: Multi-sensor infrastructure-based dataset for mobility research,” in *2022 IEEE Intelligent Vehicles Symposium (IV)*. IEEE, 2022, pp. 965–970.
- [15] T. Chavdarova, P. Baqué, S. Bouquet, A. Maksai, C. Jose, T. Bagautdinov, L. Lettry, P. Fua, L. Van Gool, and F. Fleuret, “Wildtrack: A multicamera hd dataset for dense unscripted pedestrian detection,” in *Proceedings of the IEEE/CVF Conference on Computer Vision and Pattern Recognition (CVPR)*. IEEE, 2018, pp. 5030–5039.
- [16] Z. Tang, M. Naphade, M.-Y. Liu, X. Yang, S. Birchfield, S. Wang, R. Kumar, D. Anastasiu, and J.-N. Hwang, “Cityflow: A city-scale benchmark for multi-target multi-camera vehicle tracking and re-identification,” in *Proceedings of the IEEE/CVF Conference on Computer Vision and Pattern Recognition (CVPR)*. IEEE, June 2019, pp. 8797–8806.
- [17] S. Busch, C. Koetsier, J. Axmann, and C. Brenner, “Lumpi: The leibniz university multi-perspective intersection dataset,” in *2022 IEEE Intelligent Vehicles Symposium (IV)*. IEEE, 2022, pp. 1127–1134.
- [18] Y. Nie, B. Lu, Q. Chen, Q. Miao, and Y. Lv, “Synposes: Generating virtual dataset for pedestrian detection in corner cases,” *IEEE Journal of Radio Frequency Identification*, vol. 6, pp. 801–804, 2022.
- [19] D. Li, Z. Zhang, X. Chen, and K. Huang, “A richly annotated pedestrian dataset for person retrieval in real surveillance scenarios,” *IEEE transactions on image processing*, vol. 28, no. 4, pp. 1575–1590, 2018.
- [20] S. Dávila-Soberón, A. Morales-Díaz, and M. Castelán, “A novel image dataset for detecting and classifying mobility aid users,” *Expert Systems with Applications*, vol. 293, p. 128697, 2025.

- [21] M. Kollmitz, A. Eitel, A. Vasquez, and W. Burgard, “Deep 3d perception of people and their mobility aids,” *Robotics and Autonomous Systems*, vol. 114, pp. 29–40, 2019.
- [22] J. Zhang, M. Zheng, M. Boyd, and E. Ohn-Bar, “X-world: Accessibility, vision, and autonomy meet,” in *Proceedings of the IEEE/CVF International Conference on Computer Vision*, 2021, pp. 9762–9771.
- [23] Stereolabs, “Zed 2 stereo camera,” <https://www.stereolabs.com/zed-2/>, accessed: 2025-08-04.
- [24] VideoLAN, “Vlc media player,” 2025, accessed: July 29, 2025. [Online]. Available: <https://www.videolan.org/vlc/>
- [25] S. Ren, K. He, R. Girshick, and J. Sun, “Faster r-cnn: Towards real-time object detection with region proposal networks,” 2016. [Online]. Available: <https://arxiv.org/abs/1506.01497>
- [26] X. Zhou, D. Wang, and P. Krähenbühl, “Objects as points,” in *arXiv preprint arXiv:1904.07850*, 2019.
- [27] Z. Ge, S. Liu, F. Wang, Z. Li, and J. Sun, “Yolox: Exceeding yolo series in 2021,” 2021. [Online]. Available: <https://arxiv.org/abs/2107.08430>
- [28] N. Carion, F. Massa, G. Synnaeve, N. Usunier, A. Kirillov, and S. Zagoruyko, “End-to-end object detection with transformers,” 2020. [Online]. Available: <https://arxiv.org/abs/2005.12872>
- [29] X. Zhu, W. Su, L. Lu, B. Li, X. Wang, and J. Dai, “Deformable detr: Deformable transformers for end-to-end object detection,” 2021. [Online]. Available: <https://arxiv.org/abs/2010.04159>
- [30] M. Caron, H. Touvron, I. Misra, H. Jégou, J. Mairal, P. Bojanowski, and A. Joulin, “Emerging properties in self-supervised vision transformers,” in *Proceedings of the IEEE/CVF international conference on computer vision*, 2021, pp. 9650–9660.
- [31] W. Lv, Y. Zhao, Q. Chang, K. Huang, G. Wang, and Y. Liu, “Rt-detrv2: Improved baseline with bag-of-freebies for real-time detection transformer,” 2024. [Online]. Available: <https://arxiv.org/abs/2407.17140>
- [32] MMDetection Contributors, “OpenMMLab Detection Toolbox and Benchmark,” Aug. 2018. [Online]. Available: <https://github.com/open-mmlab/mmdetection>

- [33] Y. Zhang, P. Sun, Y. Jiang, D. Yu, F. Weng, Z. Yuan, P. Luo, W. Liu, and X. Wang, “Bytetrack: Multi-object tracking by associating every detection box,” 2022. [Online]. Available: <https://arxiv.org/abs/2110.06864>
- [34] N. Aharon, R. Orfaig, and B.-Z. Bobrovsky, “Bot-sort: Robust associations multi-pedestrian tracking,” 2022. [Online]. Available: <https://arxiv.org/abs/2206.14651>
- [35] J. Cao, J. Pang, X. Weng, R. Khirodkar, and K. Kitani, “Observation-centric sort: Rethinking sort for robust multi-object tracking,” 2023. [Online]. Available: <https://arxiv.org/abs/2203.14360>
- [36] I. Loshchilov and F. Hutter, “Decoupled weight decay regularization,” in *International Conference on Learning Representations*, 2019.
- [37] T.-Y. Lin, M. Maire, S. Belongie, J. Hays, P. Perona, D. Ramanan, P. Dollár, and C. L. Zitnick, “Microsoft coco: Common objects in context,” in *European conference on computer vision (ECCV)*. Springer, 2014, pp. 740–755.
- [38] J. Luiten, A. Ošep, P. Dendorfer, P. Torr, A. Geiger, L. Leal-Taixé, and B. Leibe, “Hota: A higher order metric for evaluating multi-object tracking,” *International Journal of Computer Vision*, vol. 129, no. 2, pp. 548–578, Oct. 2020. [Online]. Available: <http://dx.doi.org/10.1007/s11263-020-01375-2>

Table 11: Tracking performance across different detectors and trackers for selected categories on video 2 test set (Part 1)

Detector	Method	Tracking Metrics (%)				Detection Counts		Track ID Counts	
		HOTA	DetA	AssA	LocA	Predictions	GT	Predictions	GT
Deformable DETR	OC-SORT	17.06	26.90	10.86	83.31	16,829		254	
CenterNet	ByteTrack	17.67	28.57	10.97	81.76	32,880		587	
CenterNet	BOT-SORT	17.75	27.93	11.33	81.73	34,088		1,239	
Faster R-CNN	OC-SORT	18.27	31.22	10.74	81.54	29,371		419	
Deformable DETR	BOT-SORT	18.32	28.36	11.89	82.77	22,584		713	
Deformable DETR	ByteTrack	18.40	28.86	11.81	82.98	21,903		392	
RT-DETR	OC-SORT	18.66	31.60	11.07	81.15	23,898		342	
Faster R-CNN	ByteTrack	18.98	29.71	12.17	81.41	34,389	17,383	482	9
Faster R-CNN	BOT-SORT	19.40	29.12	12.98	81.36	35,277		909	
CenterNet	OC-SORT	19.73	31.64	12.35	82.08	25,376		496	
RT-DETR	BOT-SORT	20.71	29.81	14.43	80.61	29,154		835	
YOLOX	OC-SORT	20.97	34.93	12.61	84.15	26,140		327	
RT-DETR	ByteTrack	<u>21.45</u>	30.49	<u>15.13</u>	80.74	28,332		485	
YOLOX	BOT-SORT	<u>23.24</u>	<u>33.40</u>	16.18	<u>83.98</u>	31,045		768	
YOLOX	ByteTrack	23.34	33.89	<u>16.09</u>	<u>84.07</u>	30,304		401	
为人									
Detector	Method	Tracking Metrics (%)				Detection Counts		Track ID Counts	
		HOTA	DetA	AssA	LocA	Predictions	GT	Predictions	GT
Faster R-CNN	OC-SORT	2.56	2.39	2.82	73.87	12,205		407	
Faster R-CNN	BOT-SORT	2.71	3.17	2.42	73.47	17,642		896	
Faster R-CNN	ByteTrack	2.75	2.98	2.65	73.88	16,717		477	
CenterNet	BOT-SORT	3.27	4.07	2.79	75.01	17,156		1,207	
CenterNet	ByteTrack	3.34	4.08	2.89	75.37	15,812		570	
CenterNet	OC-SORT	3.55	3.85	3.40	75.67	9,499		498	
YOLOX	BOT-SORT	5.09	4.32	6.10	78.57	12,966		758	
YOLOX	ByteTrack	5.16	4.26	6.34	<u>78.86</u>	12,147	7,770	399	3
Deformable DETR	OC-SORT	5.25	<u>7.47</u>	3.72	79.25	7,783		286	
RT-DETR	ByteTrack	5.40	5.77	5.25	77.39	12,648		463	
YOLOX	OC-SORT	5.52	4.02	7.63	79.78	8,536		333	
RT-DETR	OC-SORT	6.01	5.54	<u>6.85</u>	77.59	8,785		369	
RT-DETR	BOT-SORT	<u>6.90</u>	5.75	8.94	76.91	13,583		822	
Deformable DETR	BOT-SORT	<u>7.18</u>	8.32	6.21	78.45	12,964		820	
Deformable DETR	ByteTrack	7.31	8.33	<u>6.45</u>	78.43	12,196		407	
为拐杖									
Detector	Method	Tracking Metrics (%)				Detection Counts		Track ID Counts	
		HOTA	DetA	AssA	LocA	Predictions	GT	Predictions	GT
CenterNet	BOT-SORT	17.80	7.55	41.96	87.75	17,765		1,160	
CenterNet	ByteTrack	18.52	8.13	42.20	87.84	16,498		557	
RT-DETR	OC-SORT	23.22	13.47	40.12	85.00	9,699		314	
CenterNet	OC-SORT	23.34	13.01	41.89	87.98	10,139		471	
Faster R-CNN	BOT-SORT	24.46	7.54	79.51	87.22	18,034		868	
Faster R-CNN	ByteTrack	25.16	7.94	79.79	87.47	17,172		468	
RT-DETR	BOT-SORT	25.97	9.41	71.74	84.92	13,950		768	
RT-DETR	ByteTrack	26.75	9.97	71.84	85.12	13,170	1,569	442	1
Faster R-CNN	OC-SORT	28.86	10.49	79.53	87.26	12,889		390	
YOLOX	BOT-SORT	30.68	10.88	86.56	89.64	12,921		730	
YOLOX	ByteTrack	31.96	11.72	87.27	90.04	12,081		392	
Deformable DETR	BOT-SORT	35.48	15.08	83.55	88.86	9,167		640	
Deformable DETR	ByteTrack	<u>36.91</u>	<u>16.23</u>	<u>84.03</u>	<u>89.13</u>	8,539		360	
YOLOX	OC-SORT	<u>37.19</u>	<u>15.96</u>	<u>86.76</u>	<u>89.73</u>	8,785		313	
Deformable DETR	OC-SORT	43.74	22.87	83.68	88.90	5,998		201	
为轮椅									

Table 12: Tracking performance across different detectors and trackers for selected categories on video 2 test set (part 2)

Detector	Method	为人				步行		行人	
		Tracking Metrics (%)				Detection Counts		Track ID Counts	
		HOTA	DetA	AssA	LocA	Predictions	GT	Predictions	GT
CenterNet	BOT-SORT	20.84	23.22	18.87	81.35	19,178		1,182	
CenterNet	ByteTrack	21.49	24.52	18.99	81.44	17,947		570	
Deformable DETR	OC-SORT	24.84	38.82	15.96	80.66	8,357		223	
Deformable DETR	BOT-SORT	26.09	32.97	20.71	81.83	12,291		760	
CenterNet	OC-SORT	26.17	31.53	21.93	85.02	11,263		480	
Faster R-CNN	BOT-SORT	26.27	24.40	28.76	80.10	20,728		876	
Faster R-CNN	ByteTrack	26.97	25.39	29.20	83.80	19,858		470	
RT-DETR	BOT-SORT	28.66	31.03	26.73	83.25	15,267	7,390	763	5
Faster R-CNN	OC-SORT	29.27	30.08	28.99	82.06	15,450		395	
RT-DETR	ByteTrack	30.06	31.78	28.70	<i>84.86</i>	14,455		455	
YOLOX	BOT-SORT	32.02	31.24	<u>33.00</u>	81.56	16,678		765	
RT-DETR	OC-SORT	32.35	38.13	27.75	82.39	10,653		324	
Deformable DETR	ByteTrack	<u>32.80</u>	34.47	31.31	82.44	11,617		379	
YOLOX	ByteTrack	32.84	32.67	33.20	<u>83.66</u>	15,908		411	
YOLOX	OC-SORT	37.71	38.69	36.88	81.51	12,206		333	
为人									
Detector	Method	Tracking Metrics (%)				Detection Counts		Track ID Counts	
		HOTA	DetA	AssA	LocA	Predictions	GT	Predictions	GT
		RT-DETR	OC-SORT	0.00	0.00	83.29	0.00	4,620	
CenterNet	OC-SORT	0.00	0.00	83.68	0.00	6,797		459	
RT-DETR	ByteTrack	0.06	0.02	84.80	0.22	8,061		434	
RT-DETR	BOT-SORT	0.07	0.03	84.53	0.20	8,836		732	
CenterNet	ByteTrack	0.09	0.03	84.08	0.28	13,172		551	
CenterNet	BOT-SORT	0.13	0.05	82.32	0.35	14,399		1,150	
Faster R-CNN	OC-SORT	0.25	0.13	82.61	0.49	9,987		389	
YOLOX	OC-SORT	0.41	0.18	82.71	0.93	5,705	749	307	1
Faster R-CNN	BOT-SORT	0.48	0.27	82.60	0.84	15,096		857	
Faster R-CNN	ByteTrack	0.48	0.25	82.51	0.92	14,238		470	
Deformable DETR	OC-SORT	0.49	<u>0.31</u>	<u>84.60</u>	0.79	2,595		184	
YOLOX	BOT-SORT	0.57	0.24	82.84	1.36	9,784		715	
YOLOX	ByteTrack	<u>0.60</u>	0.26	<u>84.82</u>	<u>1.41</u>	9,034		387	
Deformable DETR	BOT-SORT	1.52	0.89	84.98	2.60	5,592		629	
Deformable DETR	ByteTrack	1.58	0.90	84.49	2.77	5,008		357	
为人									
Detector	Method	Tracking Metrics (%)				Detection Counts		Track ID Counts	
		HOTA	DetA	AssA	LocA	Predictions	GT	Predictions	GT
RT-DETR	BOT-SORT	9.86	3.79	81.35	26.03	9,194		731	
CenterNet	OC-SORT	4.69	3.30	81.44	6.73	6,919		460	
Deformable DETR	OC-SORT	16.45	9.58	80.66	28.68	3,438		184	
Deformable DETR	ByteTrack	<u>14.04</u>	6.78	81.83	29.64	5,917		354	
Faster R-CNN	ByteTrack	<u>13.69</u>	3.96	85.02	47.49	14,698		466	
Deformable DETR	BOT-SORT	13.09	<u>6.15</u>	80.10	28.43	6,503		624	
Faster R-CNN	BOT-SORT	13.05	3.69	83.80	46.34	15,567		854	
Faster R-CNN	OC-SORT	12.33	4.90	83.25	31.16	10,419	801	388	1
RT-DETR	OC-SORT	11.16	5.27	82.06	23.96	4,976		306	
CenterNet	ByteTrack	10.92	3.79	<i>84.86</i>	<i>31.64</i>	13,469		551	
YOLOX	OC-SORT	10.88	4.96	81.56	24.17	6,066		307	
YOLOX	ByteTrack	10.70	4.19	82.39	27.78	9,451		388	
RT-DETR	ByteTrack	10.51	4.12	82.44	27.22	8,386		434	
CenterNet	BOT-SORT	10.23	3.42	<u>83.66</u>	<u>30.70</u>	14,664		1,150	
YOLOX	BOT-SORT	10.06	3.89	81.51	26.34	10,196		717	
为人									

Table 13: Tracking performance across different detectors and trackers for selected categories on video 2 test set (part 3)

Detector	Method	Tracking Metrics (%)				Detection Counts		Track ID Counts	
		HOTA	DetA	AssA	LocA	Predictions	GT	Predictions	GT
WheelchairGroup									
CenterNet	ByteTrack	26.50	33.94	20.69	88.28	23,035		564	
CenterNet	BOT-SORT	26.64	32.20	22.04	87.80	24,156		1,224	
RT-DETR	BOT-SORT	27.95	36.58	21.37	87.02	16,572		756	
RT-DETR	ByteTrack	28.76	38.32	21.61	87.55	15,754		452	
CenterNet	OC-SORT	28.88	44.25	18.87	87.84	16,363		482	
RT-DETR	OC-SORT	32.38	44.27	23.69	87.32	11,964		329	
Deformable DETR	OC-SORT	33.22	51.20	21.59	87.76	9,871		195	
Deformable DETR	BOT-SORT	38.80	44.61	33.77	87.29	13,365	9,672	646	5
Faster R-CNN	BOT-SORT	40.13	32.84	49.04	87.92	25,414		874	
Deformable DETR	ByteTrack	40.39	46.60	35.02	87.93	12,768		366	
Faster R-CNN	ByteTrack	40.99	34.15	49.19	88.37	24,582		475	
Faster R-CNN	OC-SORT	50.91	40.98	63.25	87.95	20,121		391	
YOLOX	BOT-SORT	51.89	41.76	64.53	87.57	19,493		732	
YOLOX	OC-SORT	57.67	52.02	64.01	87.64	15,239		314	
YOLOX	ByteTrack	60.65	43.87	83.85	88.14	18,700		391	
WheelchairPusher									
Detector	Method	Tracking Metrics (%)				Detection Counts		Track ID Counts	
		HOTA	DetA	AssA	LocA	Predictions	GT	Predictions	GT
CenterNet	OC-SORT	26.41	41.01	17.01	83.21	16,259		475	
RT-DETR	BOT-SORT	26.46	32.89	21.31	82.65	15,978		767	
RT-DETR	ByteTrack	27.04	34.09	21.47	82.76	15,207		449	
CenterNet	BOT-SORT	27.16	29.59	24.94	83.17	24,449		1,239	
Deformable DETR	OC-SORT	27.20	46.06	16.08	84.19	9,338		190	
RT-DETR	OC-SORT	28.29	39.19	20.44	82.96	11,422		312	
Faster R-CNN	BOT-SORT	28.48	30.25	26.83	83.04	24,948		888	
CenterNet	ByteTrack	29.50	31.15	27.94	83.27	23,161	9,672	570	5
Faster R-CNN	OC-SORT	30.46	37.28	24.89	83.06	19,678		398	
Faster R-CNN	ByteTrack	31.17	31.41	30.93	83.27	24,070		477	
Deformable DETR	BOT-SORT	33.88	41.22	27.86	83.69	12,671		636	
Deformable DETR	ByteTrack	34.58	42.63	28.06	84.01	12,093		359	
YOLOX	BOT-SORT	38.34	39.08	37.65	84.16	18,167		727	
YOLOX	ByteTrack	38.73	40.66	36.92	84.16	17,440		391	
YOLOX	OC-SORT	41.44	47.40	36.27	84.33	14,100		318	
WheelchairPushedUser									
Detector	Method	Tracking Metrics (%)				Detection Counts		Track ID Counts	
		HOTA	DetA	AssA	LocA	Predictions	GT	Predictions	GT
CenterNet	BOT-SORT	24.87	28.97	21.49	82.16	23,723		1,184	
CenterNet	OC-SORT	27.85	38.88	20.11	82.02	15,183		468	
RT-DETR	BOT-SORT	27.88	34.09	23.25	82.46	15,772		741	
RT-DETR	ByteTrack	28.50	35.43	23.43	82.61	14,989		434	
RT-DETR	OC-SORT	30.58	41.48	23.01	82.76	11,393		307	
CenterNet	ByteTrack	32.65	30.63	34.89	82.26	22,376		556	
Deformable DETR	OC-SORT	33.88	53.49	21.48	86.09	10,169		184	
Deformable DETR	BOT-SORT	35.40	45.64	27.47	86.05	13,454	9,672	633	5
Deformable DETR	ByteTrack	36.07	47.25	27.55	86.23	12,907		357	
Faster R-CNN	BOT-SORT	42.47	30.87	58.45	82.80	24,776		863	
Faster R-CNN	ByteTrack	43.28	31.99	58.55	82.86	23,905		470	
Faster R-CNN	OC-SORT	45.54	38.25	54.21	82.80	19,635		393	
YOLOX	BOT-SORT	59.05	42.74	81.59	87.06	18,740		718	
YOLOX	ByteTrack	60.16	44.29	81.72	87.13	18,071		387	
YOLOX	OC-SORT	65.52	53.06	80.90	87.14	14,659		311	

Table 14: Tracking performance across different detectors and trackers for selected categories on video 3 test set (Part 1)

Detector	Method	Ped				Detection Counts		Track ID Counts	
		Tracking Metrics (%)				Predictions	GT	Predictions	GT
		HOTA	DetA	AssA	LocA				
CenterNet	OC-SORT	52.11	59.83	45.42	85.83	5,198		80	
Faster R-CNN	OC-SORT	52.47	62.94	43.78	85.33	4,975		53	
CenterNet	BOT-SORT	61.33	49.43	76.22	86.02	6,686		237	
RT-DETR	OC-SORT	61.36	71.75	52.66	85.99	4,501		36	
CenterNet	ByteTrack	61.91	51.32	74.82	86.05	6,436		103	
Faster R-CNN	BOT-SORT	63.66	58.37	69.48	85.38	5,589		164	
Faster R-CNN	ByteTrack	68.18	59.93	77.65	85.48	5,444		83	
YOLOX	BOT-SORT	73.25	67.84	79.35	85.24	4,735	3,995	130	5
YOLOX	ByteTrack	73.41	69.96	77.35	85.29	4,591		71	
Deformable DETR	OC-SORT	74.47	79.63	69.79	86.49	4,047		17	
YOLOX	OC-SORT	75.04	73.27	77.17	85.23	4,315		53	
RT-DETR	BOT-SORT	75.91	68.16	<u>85.12</u>	86.01	4,796		82	
RT-DETR	ByteTrack	<u>76.58</u>	69.43	85.01	86.04	4,706		40	
Deformable DETR	BOT-SORT	<u>81.99</u>	<u>78.79</u>	<u>85.48</u>	<u>86.56</u>	4,201		47	
Deformable DETR	ByteTrack	82.44	<u>79.46</u>	85.70	86.70	4,166		23	
Detector	Method	Cane				Detection Counts		Track ID Counts	
		Tracking Metrics (%)				Predictions	GT	Predictions	GT
		HOTA	DetA	AssA	LocA				
CenterNet	BOT-SORT	29.90	27.51	32.54	82.02	4,222		242	
Faster R-CNN	BOT-SORT	34.51	37.54	31.91	82.28	3,188		172	
CenterNet	ByteTrack	35.25	28.95	43.10	81.87	3,993		105	
Faster R-CNN	ByteTrack	35.41	39.37	32.02	82.28	3,028		81	
CenterNet	OC-SORT	40.17	36.36	44.53	81.99	2,864		84	
YOLOX	ByteTrack	44.17	50.85	38.58	81.67	2,193		66	
YOLOX	BOT-SORT	45.04	48.47	41.98	81.66	2,313		133	
YOLOX	OC-SORT	45.99	55.91	38.32	81.71	1,916	1,598	53	2
Faster R-CNN	OC-SORT	50.60	42.67	<u>60.05</u>	81.88	2,587		56	
RT-DETR	OC-SORT	53.44	54.64	52.30	81.67	2,065		34	
Deformable DETR	OC-SORT	56.33	<u>64.44</u>	49.39	82.94	1,532		21	
Deformable DETR	BOT-SORT	58.15	<u>63.62</u>	53.23	<u>82.60</u>	1,726		48	
Deformable DETR	ByteTrack	<u>58.66</u>	64.58	53.36	<u>82.63</u>	1,695		20	
RT-DETR	BOT-SORT	<u>60.08</u>	49.76	72.56	81.69	2,373		79	
RT-DETR	ByteTrack	61.37	51.77	72.74	81.71	2,278		38	
Detector	Method	Wheelchair				Detection Counts		Track ID Counts	
		Tracking Metrics (%)				Predictions	GT	Predictions	GT
		HOTA	DetA	AssA	LocA				
CenterNet	BOT-SORT	38.59	18.46	80.71	85.66	3,578		231	
CenterNet	ByteTrack	40.13	19.88	81.06	85.93	3,312		102	
Faster R-CNN	BOT-SORT	47.57	27.28	83.00	86.15	2,435		161	
Faster R-CNN	ByteTrack	49.09	29.06	82.97	86.07	2,283		80	
CenterNet	OC-SORT	49.12	29.64	81.42	85.76	2,184		78	
Faster R-CNN	OC-SORT	53.99	35.14	82.99	85.89	1,884		52	
YOLOX	BOT-SORT	62.45	44.71	87.25	90.63	1,537		121	
RT-DETR	BOT-SORT	62.97	44.50	89.11	90.21	1,616	799	73	1
RT-DETR	ByteTrack	64.63	46.95	88.99	90.18	1,529		36	
YOLOX	ByteTrack	65.26	48.78	87.32	90.66	1,406		67	
RT-DETR	OC-SORT	68.84	53.22	89.05	90.22	1,347		31	
YOLOX	OC-SORT	71.59	58.73	87.26	90.63	1,160		50	
Deformable DETR	BOT-SORT	<u>78.31</u>	68.79	<u>89.15</u>	<u>91.45</u>	1,023		42	
Deformable DETR	ByteTrack	<u>79.76</u>	<u>71.02</u>	89.59	91.66	992		20	
Deformable DETR	OC-SORT	82.75	76.64	<u>89.34</u>	<u>91.51</u>	913		15	

Table 15: Tracking performance across different detectors and trackers for selected categories on video 3 test set (part 2)

Detector	Method	Tracking Metrics (%)				Detection Counts		Track ID Counts	
		HOTA	DetA	AssA	LocA	Predictions	GT	Predictions	GT
$\ddot{\text{f}}$ WalkerWalking									
CenterNet	ByteTrack	1.17	0.38	3.58	82.30	3,127		102	
CenterNet	BOT-SORT	1.17	0.36	3.78	84.41	3,443		234	
CenterNet	OC-SORT	1.30	0.61	2.80	84.77	2,092		80	
Deformable DETR	BOT-SORT	1.51	1.28	1.78	86.32	737		43	
Deformable DETR	ByteTrack	1.57	<u>1.36</u>	1.81	87.38	707		20	
Faster R-CNN	BOT-SORT	1.71	0.74	3.98	80.50	1,696		162	
YOLOX	ByteTrack	1.76	1.11	2.78	83.71	1,106		69	
Faster R-CNN	ByteTrack	1.80	0.81	4.00	80.76	1,541	16	80	1
RT-DETR	OC-SORT	1.82	0.98	3.45	83.99	1,366		31	
Faster R-CNN	OC-SORT	2.08	1.09	3.96	80.02	1,135		54	
YOLOX	OC-SORT	2.12	<u>1.52</u>	2.97	87.40	870		50	
YOLOX	BOT-SORT	2.24	1.06	4.73	86.70	1,229		123	
Deformable DETR	OC-SORT	<u>4.56</u>	1.53	<u>13.58</u>	<u>86.62</u>	617		16	
RT-DETR	BOT-SORT	<u>4.82</u>	0.81	<u>29.11</u>	83.98	1,641		79	
RT-DETR	ByteTrack	5.08	0.89	29.54	83.98	1,503		41	
$\ddot{\text{f}}$ WalkerResting									
Detector	Method	Tracking Metrics (%)				Detection Counts		Track ID Counts	
		HOTA	DetA	AssA	LocA	Predictions	GT	Predictions	GT
RT-DETR	OC-SORT	26.96	36.39	20.19	80.69	1,106		32	
CenterNet	BOT-SORT	44.62	30.32	65.96	80.56	3,641		231	
CenterNet	ByteTrack	46.04	32.05	66.40	80.73	3,420		104	
Deformable DETR	OC-SORT	46.43	53.39	40.63	88.00	1,110		16	
RT-DETR	ByteTrack	48.67	37.11	64.17	80.51	1,446		36	
RT-DETR	BOT-SORT	48.79	36.95	64.76	80.38	1,485		80	
YOLOX	BOT-SORT	49.90	39.16	63.71	83.11	1,600		122	
YOLOX	ByteTrack	51.16	40.94	64.02	83.24	1,473	1,582	66	2
Faster R-CNN	BOT-SORT	51.77	38.86	69.33	85.18	3,003		161	
CenterNet	OC-SORT	52.76	47.50	59.34	80.60	2,202		79	
Faster R-CNN	ByteTrack	52.99	40.70	69.37	85.25	2,853		80	
YOLOX	OC-SORT	53.65	43.41	66.38	83.50	1,208		50	
Faster R-CNN	OC-SORT	<u>56.48</u>	46.13	<u>69.48</u>	<u>85.36</u>	2,441		52	
Deformable DETR	BOT-SORT	<u>60.17</u>	<u>51.14</u>	71.12	<u>87.85</u>	1,264		44	
Deformable DETR	ByteTrack	60.67	52.05	<u>71.04</u>	88.00	1,222		20	

Table 16: Tracking performance across different detectors and trackers for selected categories on video 3 test set (part 3)

Detector	Method	WheelchairGroup				Detection Counts		Track ID Counts	
		Tracking Metrics (%)				Predictions	GT	Predictions	GT
		HOTA	DetA	AssA	LocA				
CenterNet	ByteTrack	35.42	29.73	42.34	85.70	4,351		102	
CenterNet	OC-SORT	36.22	40.31	32.66	86.92	3,196		84	
CenterNet	BOT-SORT	38.02	28.52	50.70	86.72	4,660		247	
Faster R-CNN	BOT-SORT	62.82	44.08	89.53	<u>90.32</u>	3,258		163	
Faster R-CNN	ByteTrack	63.77	45.82	88.75	89.91	3,108		82	
Faster R-CNN	OC-SORT	68.27	52.30	89.11	90.26	2,720		55	
YOLOX	BOT-SORT	71.12	57.05	88.66	89.32	2,480		132	
YOLOX	OC-SORT	72.44	66.14	79.40	89.27	2,076	1,598	52	2
RT-DETR	BOT-SORT	72.52	58.91	<u>89.29</u>	89.80	2,422		75	
YOLOX	ByteTrack	72.58	60.02	87.78	88.83	2,338		72	
RT-DETR	ByteTrack	73.44	60.75	88.78	89.50	2,335		38	
RT-DETR	OC-SORT	76.72	66.01	89.17	89.81	2,151		33	
Deformable DETR	OC-SORT	<u>77.77</u>	81.83	73.98	<u>90.41</u>	1,709		17	
Deformable DETR	BOT-SORT	<u>83.38</u>	<u>77.58</u>	89.61	90.56	1,842		46	
Deformable DETR	ByteTrack	83.49	78.39	88.93	90.02	1,808		21	
WheelchairPusher									
Detector	Method	WheelchairPusher				Detection Counts		Track ID Counts	
		Tracking Metrics (%)				Predictions	GT	Predictions	GT
		HOTA	DetA	AssA	LocA				
CenterNet	BOT-SORT	31.90	29.48	34.53	85.47	4,466		243	
CenterNet	OC-SORT	34.66	42.94	28.00	85.47	2,920		80	
Faster R-CNN	OC-SORT	35.08	48.03	25.69	86.33	2,687		53	
YOLOX	BOT-SORT	40.05	54.77	29.33	85.80	2,372		126	
YOLOX	ByteTrack	41.23	57.88	29.40	85.80	2,240		68	
Faster R-CNN	BOT-SORT	48.50	40.85	57.60	<u>86.30</u>	3,287		163	
Faster R-CNN	ByteTrack	49.72	42.84	57.74	86.33	3,129		81	
CenterNet	ByteTrack	49.92	30.96	80.53	85.46	4,242	1,598	102	2
RT-DETR	BOT-SORT	55.86	54.77	57.04	85.47	2,405		77	
RT-DETR	ByteTrack	56.87	56.69	57.11	85.49	2,323		37	
RT-DETR	OC-SORT	58.15	60.22	56.21	85.69	2,109		34	
YOLOX	OC-SORT	67.54	64.43	<u>70.85</u>	85.81	1,955		53	
Deformable DETR	BOT-SORT	<u>69.24</u>	<u>71.19</u>	67.41	<u>86.26</u>	1,825		45	
Deformable DETR	OC-SORT	<u>70.12</u>	74.09	66.46	86.33	1,664		17	
Deformable DETR	ByteTrack	70.54	72.27	68.93	86.08	1,786		22	
WheelchairPushedUser									
Detector	Method	WheelchairPushedUser				Detection Counts		Track ID Counts	
		Tracking Metrics (%)				Predictions	GT	Predictions	GT
		HOTA	DetA	AssA	LocA				
CenterNet	OC-SORT	40.23	42.93	37.78	85.85	2,925		82	
CenterNet	BOT-SORT	44.14	30.28	64.36	85.74	4,376		235	
CenterNet	ByteTrack	45.10	32.15	63.28	85.52	4,119		102	
Faster R-CNN	BOT-SORT	59.53	41.22	86.00	87.48	3,354		161	
Faster R-CNN	ByteTrack	60.93	43.18	85.98	87.49	3,200		80	
Faster R-CNN	OC-SORT	64.21	48.87	84.39	87.45	2,782		53	
YOLOX	OC-SORT	67.35	68.75	66.02	87.86	2,007		52	
RT-DETR	BOT-SORT	69.49	56.19	85.96	87.31	2,440	1,598	74	2
RT-DETR	ByteTrack	70.80	58.34	85.95	87.26	2,351		38	
YOLOX	BOT-SORT	71.14	58.00	87.29	87.86	2,401		121	
YOLOX	ByteTrack	73.00	61.23	<u>87.04</u>	87.77	2,268		67	
RT-DETR	OC-SORT	73.71	63.19	86.00	87.30	2,167		33	
Deformable DETR	BOT-SORT	<u>80.53</u>	74.96	<u>86.52</u>	88.27	1,837		43	
Deformable DETR	ByteTrack	<u>81.06</u>	76.11	86.34	<u>88.23</u>	1,806		21	
Deformable DETR	OC-SORT	82.48	79.17	85.94	<u>88.11</u>	1,719		15	